


# Titania sensitized with SPADNS dye for dye sensitized solar cell

Pravin N. Didwal<sup>1</sup> · Kalpana S. Pawar<sup>1</sup> · Parameshwar R. Chikate<sup>1</sup> ·  
Ashutosh C. Abhyankar<sup>2</sup> · Habib M. Pathan<sup>1</sup> · Rupesh S. Devan<sup>1,3</sup> 

Received: 28 April 2016 / Accepted: 25 July 2016 / Published online: 2 August 2016  
© Springer Science+Business Media New York 2016

**Abstract** Synthesis of anatase TiO<sub>2</sub> nanoparticle with diameter about 25 nm is carried out by using chemical method and powder of TiO<sub>2</sub> nanoparticle is pasted on fluorine doped tin oxide (FTO) coated glass by doctor blade. New organic SPADNS dye (C<sub>16</sub>H<sub>9</sub>N<sub>2</sub>Na<sub>3</sub>O<sub>11</sub>S<sub>3</sub>) is used first time to make the dye-sensitized solar cells (DSSC). Cell were constructed by using SPADNS dye loaded wide band gap anatase TiO<sub>2</sub> nanoparticle on FTO coated glass as photo-anode, polyiodide as electrolyte, and platinum coated FTO as counter electrode. SPADNS dye was made from organic reagent which is low cost and easy available in market. Better adsorption of SPADNS dye on anatase TiO<sub>2</sub> film is due to porous nature of TiO<sub>2</sub>. This better adsorption gives more transportation of electron from dye to TiO<sub>2</sub> which increase the efficiency of solar cell. Although SPADNS dye is the first experiment with TiO<sub>2</sub> nanoparticle for DSSC, it gives photocurrent (short-circuit current density) 1.04 mA/cm<sup>2</sup>, open-circuit voltage 0.59 V, with 0.9 % efficiency under 10 mW/m<sup>2</sup> LED.

## 1 Introduction

Dye sensitized solar cells (DSSC) are found to provide relatively high efficiency and have low fabrication cost; could be an important alternative for conventional silicon solar cells [1]. The DSSC is invented by O'Regan and Grätzel in 1991, consists of four important components, such as electrolyte, a photo-anode, counter electrode and dye. In spite of their excellent performance, several limitations such as (1) installation area, (2) location as well as availability of sun radiation, (3) initial cost, (4) pollution, (5) less efficiency, and (6) reliability are holding their commercialization and large scale applications in technological scenario. Utilization of various dimensional nanomaterial such as nanoplates, nanoparticles [2–4], nanowires [5, 6], nanorods [5, 7], and nanotubes [5–11], etc. for the fabrication of DSSC can help partially to solve the limitations afford by DSSC so far Semiconductor has vital role in the absorption of the sunlight, transportation of charge and antireflection coating for solar cell [12]. Wide band gap semiconductor nanomaterial used as photo electrode in DSSC [13, 14]. Main role of the absorption of the sunlight in visible region and injection of charge into the semiconducting material plays by sensitizer. Various type of sensitizer is used to increase the efficiency of the cell such as organic [15–17], hybrid compound [18] and natural [19, 20] etc. Ruthenium inorganic dyes are mostly used as molecular sensitizer in DSSC which having high efficiency up to 11 % [21, 22] but is very costly and thus cost of the solar cell becomes high with ruthenium dye. Natural dye is not so pricey and easy extraction but it gives very low efficiency than other sensitizer. Thus there is significant interest in that sensitizer which is not so expensive with good efficiency.

✉ Rupesh S. Devan  
devan\_rs@yahoo.co.in

Habib M. Pathan  
pathan@physics.unipune.ac.in

<sup>1</sup> Department of Physics, Savitribai Phule Pune University (Formerly, University of Pune), Ganeshkhind, Pune 411007, India

<sup>2</sup> Department of Materials Engineering, Defence Institute of Advanced Technology, Pune 411025, India

<sup>3</sup> Centre for Physical Sciences, School of Basic and Applied Sciences, Central University of Punjab, Bhatinda, Punjab 151001, India

In this work, anatase phase of TiO<sub>2</sub> metal oxide is used as photo-electrode and organic dye as absorber material. SPADNS dye is made from the spadns inorganic reagent which is cheaper, easy available everywhere, gives good amount of yield and not degrade at low intensity. The performance of more organic dyes with titania are studied mostly for solar cell application [23] but this SPADNS organic dye is use first time in DSSC. Among all transition metal oxides, TiO<sub>2</sub> is the most studied material as it exhibits a broad range of functional properties. TiO<sub>2</sub> is a white solid and inorganic substance which is non-flammable, thermally stable, nonhazardous, and poorly soluble in organic as well as inorganic solvent [24, 25]. These variety of TiO<sub>2</sub> nanostructures have received plenty of attention for their wide spread applications in cosmetics, pigmentation [24], batteries [26, 27], supercapacitor [28, 29], solar cells [13, 14], hydrogen evolution [30, 31], self cleaning, antireflecting coating [32] and field emitters [33, 34]. Due to wide band gap range, high refractive index, good chemical as well as thermal stability, various dimensional nanostructure of TiO<sub>2</sub> have been widely use in energy saving application and convenient visual environment. The transparent nature of TiO<sub>2</sub> nanomaterials (ultrafine) guided for their more effective use as photocatalysts or ultraviolet absorbers. Since then, huge efforts have been made to the research on TiO<sub>2</sub> nanomaterial, which has accompany to many applications in areas ranging from photocatalysis and photovoltaics to sensors and photo-electrochromics [35]. These huge applications can be divided into environmental and energy categories. The many applications depend not only on the interactions of TiO<sub>2</sub> materials with the environment, but also on the morphological features of the TiO<sub>2</sub> material itself. UV–Vis spectroscopy is used to observe the absorption of SPADNS dye alone and titania sensitized with SPADNS dye in visible region. Photo-anode is made with TiO<sub>2</sub> nanoparticle pasted on FTO coated glass by method of doctor blading and then sensitized with SPADNS dye. Solar cell is fabricated by sandwich of dye loaded TiO<sub>2</sub> photo-anode and platinum coated FTO glass substrate and photo electrochemical properties are calculated under the influence of solar radiation.

## 2 Experimental

TiO<sub>2</sub> nanoparticles were synthesized with titanium trichloride (TiCl<sub>3</sub>) as a precursor and sodium hydroxide (NaOH) as reducing agent using chemical method at room temperature [36]. After reaction of TiCl<sub>3</sub> and NaOH, white precipitation was formed. The precipitate solution was stirrer further for few hours and filtered. After heating the filtrate at temperature of 60 °C, white powder of TiO<sub>2</sub>

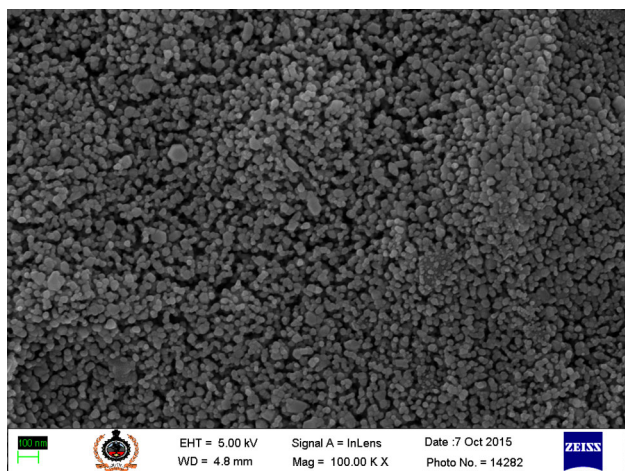
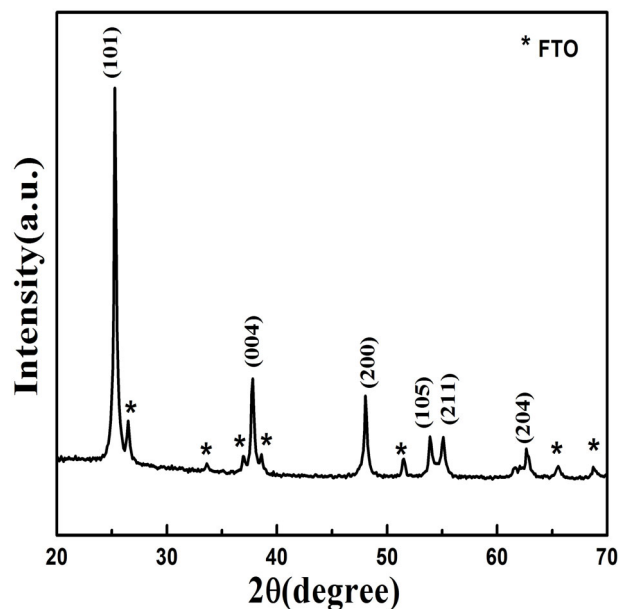
formed. Formation of dens Anatase TiO<sub>2</sub> porous nanoparticle film on transparent conducting oxide FTO substrate is carried out by doctor blade explained elsewhere [37]. SPADNS (C<sub>16</sub>H<sub>9</sub>N<sub>2</sub>Na<sub>3</sub>O<sub>11</sub>S<sub>3</sub>, 3, 6-disulphonic acid, 1, 8-dihydroxy naphthalene, tri-sodium salt) reagent was purchased from sigma Aldrich (99.9 %). A 0.5 mM dye solution was prepared in ethyl alcohol by using red color spadns reagent. TiO<sub>2</sub> films after preparing at room temperature were coated with sensitizing SPADNS dye overnight. Highly conducting platinized counter electrode was prepared by sputtering technique on transparent conducting oxide FTO- coated glass. Structural and optical properties of dye loaded TiO<sub>2</sub> porous nanoparticle thin film were characterize using XRD (Bruker AXS D8, Cu K<sub>α</sub>, λ = 1.54 Å) and UV–Vis spectroscopy (Jasco V-670), respectively. Size and porosity of the TiO<sub>2</sub> nano-particle were obtained from Field Emission Scanning Electron Microscopy (FESEM). Chemical compositional analysis was carried out by Fourier Transform Infra Red spectroscopy (FT-IR). The active area of the cell is about 0.25 cm<sup>2</sup>. To find the efficiency and fill factor of dye loaded TiO<sub>2</sub> porous nano-particle film, J–V characteristic were carried out.

## 3 Results and discussion

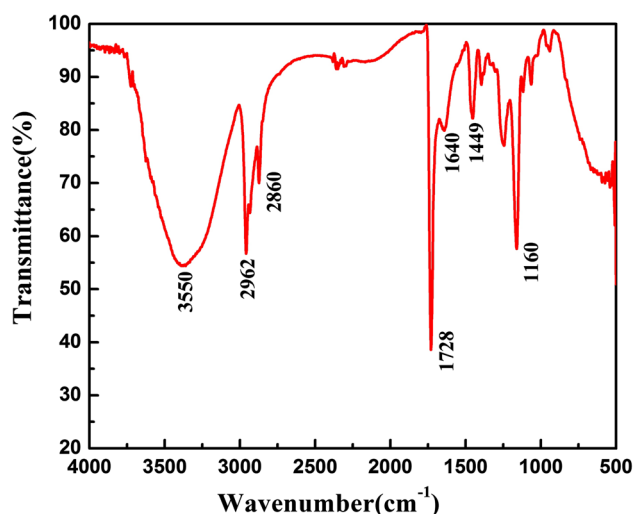
X-ray diffraction pattern of TiO<sub>2</sub> nano-particle deposited on fluorine doped tin oxide (FTO) substrate by using doctor blade is shown in Fig. 1. The synthesized TiO<sub>2</sub> nanoparticles are of tetragonal crystals (JCPDS card no. 04-0477), assigned to the space group 141/amd with lattice contacts a = 3.783 Å, b = 3.783 Å, c = 9.51 Å and α = 90°, β = 90°, γ = 90° This diffraction peaks at 2θ angle 25.29°, 37.79°, 48.01°, 53.91°, 55.06° and 62.57° corresponding to (101), (004), (200), (105), (211) and (204) plans confirms anatase phase and the crystalline nature of TiO<sub>2</sub>. This confirms that there is not formation of another phase like rutile or brookite. Low intense peaks indicating by asterisk are assigned to the conducting FTO of monoclinic crystal in the space group of C2/m with lattice constant a = 9.296 Å, b = 8.076 Å, c = 5.074 Å and α = 90°, β = 97.9°, γ = 90° (JCPDS card no. 25-0875). The crystalline size of the prepared anatase TiO<sub>2</sub> was calculated from Debye Scherer equation [38]. The average crystallite size of TiO<sub>2</sub> nano-particle was around 20 nm.

Figure 2 shows the FESEM image of TiO<sub>2</sub> nano-particles pasted on the FTO substrate. Close inspection of the FESEM images shows that the pure TiO<sub>2</sub> nano-particles have irregular shape. The particles of anatase TiO<sub>2</sub> are uniformly distributed over the FTO substrate. Size of the particle varies from 11 to 38 nm, with average particle size around 25 nm. The arrangement of TiO<sub>2</sub> nano-particle on

**Fig. 1** XRD spectrum of TiO<sub>2</sub> nanoparticles on FTO coated glass substrate



**Fig. 2** FESEM image showing top view of TiO<sub>2</sub> nanoparticle coated on FTO coated glass substrate



**Fig. 3** FTIR spectrum of SPADNS dye loaded TiO<sub>2</sub> nanoparticle

FTO shows the porous nature of film, which provides the larger adsorption surface for dye molecule and enhance the performance of solar cell [39–41].

Fourier transformed infrared spectroscopy is a favorable method to observe the molecular vibration of composite. The FTIR spectrum shown in the Fig. 3 reveal most of the characteristic peaks of the SPADNS dye loaded on the TiO<sub>2</sub> particle film. The C–H symmetric stretching modes attributes by two peaks observed at 2962 and 2860 cm<sup>-1</sup>. Absorption peak having broad range between 3200 and 3550 cm<sup>-1</sup> indicates O–H stretching vibration. The broad absorption in this spectrum observed due to presence of

alcoholic group and phenolic group in the SPADNS dye. The ultra sharp peak at wave number 1728 cm<sup>-1</sup> is in conformity with C=O bonding of the dihydroxy naphthalene. Peak at 1449 and 1160 cm<sup>-1</sup> are arise mainly due to C–C and C–N bond vibration mode of the sulphonic acid and benzene ring of azo benzene respectively [42]. Peak at 1640 cm<sup>-1</sup> shows C=C stretching vibration. Overall, the sharp peaks observed of C–N and C=O bonds are indicative of the good adsorption of SPADNS dye on porous TiO<sub>2</sub> film. This indicates that, interacting surface area of the TiO<sub>2</sub> nanoparticle has large with molecules of SPADNS dye.

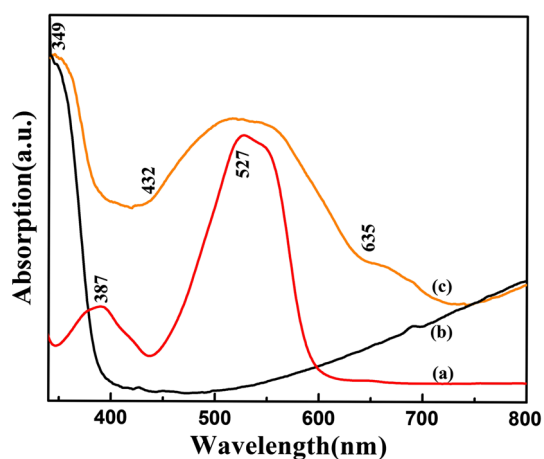


**Fig. 4** UV-Vis absorption spectra of **a** SPADNS dye (red in color), **b** pure TiO<sub>2</sub> (black in color), and **c** SPADNS dye loaded on TiO<sub>2</sub> nanoparticle (orange in color) (Color figure online)

The optical absorption spectrum of SPADNS dye, pure TiO<sub>2</sub> and SPADNS dye loaded on TiO<sub>2</sub> as shown in the Fig. 4. Figure shows the significant difference between the absorption of the SPADNS dye and dye loaded on TiO<sub>2</sub> in visible region. Figure 4a shows Absorption spectra of the dye with two broad absorption peaks in the visible region, first absorption peak at maximum 527 nm and second at 387 nm and this maximum responsible for attractive red color of the SPADNS dye. Figure 4b shows absorption spectra of pure TiO<sub>2</sub>. Absorption edge occur around 349 nm which indicates that TiO<sub>2</sub> absorbed radiations in ultra-violet region. Figure 4c shows the interaction of the SPADNS dye with TiO<sub>2</sub> nanoparticles and combines effect obtained from the absorption spectra. The broad absorption spectra form 432 to 635 nm in the dye loaded TiO<sub>2</sub> film confirmed that anchoring of the dye with the surface of

TiO<sub>2</sub>. Absorption of SPADNS dye loaded TiO<sub>2</sub> nanoparticles is better in visible region. The transformation of the electron from dye molecules to semiconductor depends on the surface interaction of dye with semiconductor material [43–45]. The surface interaction of SPADNS dye with TiO<sub>2</sub> nanoparticles is very important to increase the performance of the efficient solar cells. Optical absorption in TiO<sub>2</sub> nanoparticles and the SPADNS dye is more due to organic element present in the dye [46]. This will help to produce better electron injection. The broadness of the absorption level of dye sensitize TiO<sub>2</sub> are influence by MLCT transition in visible region [47].

Performance of the solar cell is calculated by using graph of current density and voltage under visible light. SPADNS dye sensitized TiO<sub>2</sub> solar cells were tested for the purpose to calculate the light to power conversion efficiency and to make the energy saving application. Although dye effect on the charge transportation, electrolyte always play the main role in the performance of the DSSC [48, 49]. Photovoltaic performance of various TiO<sub>2</sub> morphologies in well known organic dye is provided in the Table 1. Moreover, Jayaweera et al. [50] have introduced photovoltaic properties of ion-associated complexes between SPADNS and rhodamine B (RhB) absorbed on TiO<sub>2</sub> surface. Efforts were added on the optimization RhB content to gain the higher photo conversion efficiency and not on SPADNS. Therefore in present study, the SPADNS organic dyes and polyiodide were used as sensitizer and electrolyte to construct the solar cell respectively. Solar cell was characterized under 10 mW/m<sup>2</sup> LED light with expose area 0.25 cm<sup>2</sup>. Figure 5 shows the current density versus voltage plot of SPADNS dye loaded TiO<sub>2</sub> film. ‘SPADNS’ dye adsorbed on TiO<sub>2</sub> film gives power conversion efficiency of 0.9 % at short circuit current

**Table 1** Photovoltaic performance of various well known organic dye and TiO<sub>2</sub> based dye sensitized solar cell

Dye code	J <sub>sc</sub> (mA/cm <sup>2</sup> )	V <sub>oc</sub> (V)	FF	η (%)	References
TA-st-CA	18.1	0.74	0.67	9.1	[15]
MK-2	14.00	0.74	0.74	7.7	[16]
JK-45	16.13	0.64	0.71	7.42	[17]
JK-46	17.45	0.66	0.74	8.6	[17]
SCZ-1	19.85	0.76	0.68	10.4	[21]
SCZ-2	19.88	0.76	0.67	10.2	[21]
N719	18.77	0.76	0.69	9.9	[21]
Indoline (D102)	07.50	0.85	0.60	4.1	[46]
N719	10.31	0.70	0.43	3.16	[45]
Indoline 1	18.75	0.64	0.53	6.51	[53]
Indoline 2	17.50	0.58	0.53	5.50	[53]
Indoline 3	17.38	0.62	0.51	5.60	[53]
Indoline 4	19.56	0.50	0.53	5.93	[53]
N3	18.06	0.69	0.62	7.89	[53]
N719	16.68	0.75	0.65	8.26	[53]

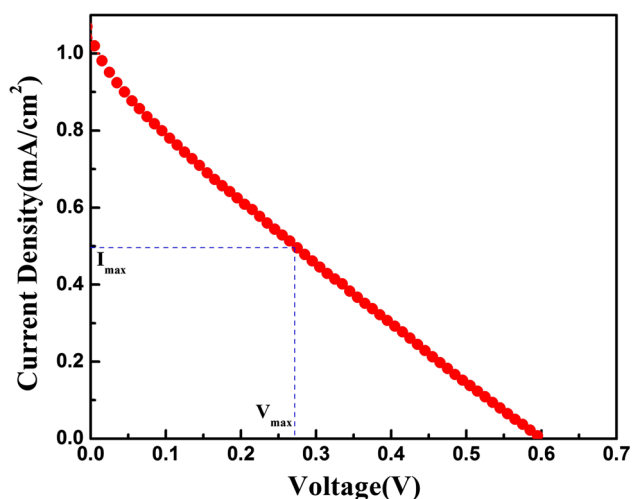


**Fig. 5** Photocurrent density–Voltage curve of Spands dye loaded  $\text{TiO}_2$  nanoparticle based DSSC

1.04  $\text{mA}/\text{cm}^2$ , open circuit voltage 0.59 V, and fill factor of 0.21. The electrical as well as electrochemical losses of dye sensitized solar cell are defined by Fill factor (FF). Efficiency of the dye sensitized solar cell can conclude by specific functional group present in the dye [51, 52]. Alcoholic ( $-\text{OH}$ ) groups present in the SPADNS dye help to enhance the efficiency of solar cell. This alcoholic group form bond with the surface of the semiconductor material and thus help to transfer electron from dye molecule to the semiconductor and give better effect in the power conversion efficiency of dye sensitized solar cell [53, 54].

#### 4 Conclusion

In this work, solution of SPADNS dye is made from organic SPADNS reagent. To utilize the solar cell,  $\text{TiO}_2$  nanoparticles are sensitized with SPADNS dye overnight and cells were tested under  $10 \text{ mW}/\text{m}^2$  LED. Crystalline nature of the  $\text{TiO}_2$  nanoparticles was confirmed from the XRD pattern.  $\text{TiO}_2$  nanoparticles show the poly-crystalline nature and anatase phase at room temperature. Zero dimensional morphology and particle size about 25 nm confirms from the field emission scanning electron microscopy. Irregular shape of the  $\text{TiO}_2$  nanoparticle has uniformly distributed over the fluorine doped tin oxide coated glass substrate. The surface interaction of  $\text{TiO}_2$  nanoparticles with SPADNS dye observed by Fourier transforms infra-red spectroscopy which concludes the transformation of the electrons to the semiconductor material from dye molecules. The change in optical absorption of pure SPADNS dye and after SPADNS dye loaded on  $\text{TiO}_2$  nanoparticle observed from ultraviolet–visible spectroscopy. Absorption of SPADNS dye become broad in

visible region after loaded on  $\text{TiO}_2$  film. This will help to increase quality of solar cell as well as power conversion efficiency. SPADNS dye gives fill factor ( $ff$ ) of 0.21 and efficiency ( $\eta$ ) of 0.90 % with short circuit current ( $I_{sc}$ )  $1.04 \text{ mA}/\text{cm}^2$  and open circuit voltage ( $V_{oc}$ ) 0.59 V.

**Acknowledgments** The authors would like to thank the Department of Science and Technology (DST), Ministry of Science and Technology of India, for their financial support of this research under INSPIRE Faculty Award No. DST/INSPIRE Faculty Award/2013/IFA13-PH-63.

#### References

1. B. O'Regan, M. Grätzel, *Nature* **353**, 7371–7740 (1991)
2. K.G. Deepa, P. Lekha, S. Sindhu, *Sol. Energy* **86**, 326–330 (2012)
3. A. Ranga Rao, V. Dutta, *Nanotechnology* **19**, 44 (2008)
4. J. Li, X. Chen, N. Ai, J. Hao, Q. Chen, S. Strauf, Y. Shi, *Chem. Phys. Lett.* **514**, 141–145 (2011)
5. H.-S. Kim, J.-W. Lee, N. Yantara, P.P. Boix, S.A. Kulkarni, S. Mhaisalkar, M. Grätzel, N. Park, *Nano Lett.* **13**(6), 2412–2417 (2013)
6. B. Pradhan, S.K. Batabyal, A.J. Pal, *Sol. Energy Mater. Sol. Cells* **91**, 769–773 (2007)
7. R.S. Devan, R.A. Patil, J.-H. Lin, Y.-R. Ma, *Adv. Funct. Mater.* **22**, 3326–3370 (2012)
8. J.B. Baxter, E.S. Aydil, *Appl. Phys. Lett.* **86**, 053114 (2005)
9. C.Y. Jiang, X.W. Sun, K.W. Tan, G.Q. Lo, A.K.K. Kyaw, D.L. Kwong, *Appl. Phys. Lett.* **92**, 143101 (2008)
10. J.H. Park, T.-W. Lee, M.G. Kang, *Chem. Commun.* **25**, 2867–2869 (2008)
11. G.K. Mor, O.K. Varghese, M. Paulose, K. Shankar, C.A. Grimes, *Sol. Energy Mater. Sol. Cells* **90**, 2011–2075 (2006)
12. R.J. Stirn, Y.C.M. Yeh, *Appl. Phys. Lett.* **27**, 95 (1975)
13. D.E. Scaife, *Sol. Energy* **25**, 41–54 (1980)
14. M.A. Butler, D.S. Ginley, *J. Mater. Sci.* **15**, 1–19 (1980)
15. S. Hwang, J.H. Lee, C. Park, H. Lee, C. Kim, C. Park, M.-H. Lee, W. Lee, J. Park, K. Kim, N.-G. Park, C. Kim, *Chem. Commun.* **46**, 4887–4889 (2007)
16. N. Koumura, Z.-S. Wang, S. Mori, M. Miyashita, E. Suzuki, K. Hara, *J. Am. Chem. Soc.* **128**, 14256–14257 (2006)
17. H. Choi, C. Baik, S.O. Kang, J. Ko, M.-S. Kang, Mdk Nazeeruddin, M. Gratzel, *Angew. Chem. Int. Ed.* **47**, 327–330 (2008)
18. B. Lim, G.Y. Margulis, J.-H. Yum, E.L. Unger, B.E. Hardin, M. Gratzel, M.D. McGehee, A. Sellinger, *Org. Lett.* **15**(4), 784–787 (2013)
19. N.A. Ludin, A.M. Al-Alwani Mahmoud, A.B. Mohamad, A.A.H. Kadhum, K. Sopian, N.S.A. Karim, *Renew. Sustain. Energy Rev.* **31**, 386–396 (2014)
20. J. Gong, J. Liang, K. Sumathy, *Renew. Sustain. Energy Rev.* **16**, 5848–5860 (2012)
21. Z. She, Y. Cheng, L. Zhang, X. Li, D. Wu, Q. Guo, J. Lan, R. Wang, J. You, *ACS Appl. Mater. Interfaces* **7**, 27831–27837 (2015)
22. C.-Y. Chen, S.-J. Wu, C.-G. Wu, J.-G. Chen, K.-C. Ho, *Angew. Chem.* **118**, 5954–5957 (2006)
23. A. Mishra, M.K.R. Fischer, P. Bauerle, *Angew. Chem. Int. Ed.* **48**, 2474–2499 (2008)
24. K. Schilling, B. Bradford, D. Castelli, E. Dufour, J.F. Nash, W. Pape, S. Schulte, I. Tooley, J. van den Bosch, F. Schellauf, *Photochem. Photobiol. Sci.* **9**, 495–509 (2010)

25. N.A. Monteiro-Riviere, K. Wiench, R. Landsiedel, S. Schulte, A.O. Inman, J.E. Riviere, *Toxicol. Sci.* **123**, 264–280 (2011)
26. S.-J. Kim, M.-C. Kim, D.-H. Kwak, D.-M. Kim, G.-H. Lee, H.-S. Choe, K.-W. Park, *J. Power Sour.* **304**, 119–127 (2016)
27. D. Deng, M.G. Kim, J.Y. Lee, J. Cho, *Energy Environ. Sci.* **2**, 818–837 (2009)
28. L. Zheng, C. Wang, Y. Dong, H. Biana, T.F. Hung, J. Lud, Y. Yang, *Appl. Surf. Sci.* **362**, 399–405 (2016)
29. Q. Wang, Z. Wen, J. Li, *Adv. Funct. Mater.* **16**, 2141–2146 (2006)
30. D.P. Kumar, N.L. Reddy, B. Srinivas, V. Durgakumari, V. Roddatis, O. Bondarchuk, M. Karthik, Y. Ikuma, M.V. Shankar, *Sol. Energy Mater. Sol. Cells* **146**, 63–71 (2016)
31. B. Wu, D. Liu, S. Mubeen, T.T. Chuong, M. Moskovits, G.D. Stucky, *J. Am. Chem. Soc.* **138**, 1114–1117 (2016)
32. P. Spinelli, B. Macco, M.A. Verschuuren, W.M.M. Kessels, A. Polman, *Appl. Phys. Lett.* **102**, 233902 (2013)
33. C.-W. Wang, J.-B. Chen, L.-Q. Wang, Y.-M. Kang, D.-S. Li, F. Zhou, *Thin Solid Films* **520**, 5036–5041 (2012)
34. J. Liang, G. Zhang, *Appl. Mater. Interfaces* **4**, 6053–6061 (2012)
35. Y.L. Xia, L.S. Lian, C.Q. Yun, Y.S. Zhuo, *Chin. Sci. Bull.* **55**, 4–5 (2010)
36. M.B. Prasad, H.M. Pathan, *Eur. Phys. J. D* **68**, 25 (2014)
37. G. Ruani, C. Ancora, F. Corticelli, C. Dionigi, C. Rossi, *Sol. Energy Mater. Sol. Cells* **92**, 537–542 (2008)
38. J.I. Langford, A.J.C. Wilson, *J. Appl. Cryst.* **11**, 102–113 (1978)
39. D. Sengupta, B. Mondal, K. Mukherjee, *Spectrochim. Acta Part A Mol. Biomol. Spectrosc.* **148**, 85–92 (2015)
40. H.H.T. Vu, T.S. Atabaev, D.P. Cong, M.A. Hossain, D. Lee, N.N. Dinh, C.R. Cho, H.K. Kim, Y.H. Hwang, *Electrochim. Acta* **193**, 166–171 (2016)
41. R.S. Mane, W.J. Lee, H.M. Pathan, S.H. Han, *J. Phys. Chem. B* **109**, 24254–24259 (2005)
42. R.M. Silverstein, F.X. Webster, *Spectrometric Identification of Organic Compound*, vol. 3 (Wiley, New York, 1998), pp. 170–230
43. Y. Liao, J. Hu, C. Zhu, Y. Liu, X. Chen, C. Chen, C. Zhong, *J. Mol. Struct.* **1108**, 467–474 (2016)
44. M. Gratzel, *J. Photochem. Photobiol. C Photochem. Rev.* **4**, 145–153 (2003)
45. U. Mehmood, I.A. Hussein, A.A. Ahmed, S. Ahmed, *J. Photovolt* **6**, 2 (2016)
46. L. Schmidt-Mende, U. Bach, R. Humphry-Baker, T. Horiuchi, H. Miura, S. Ito, S. Uchida, M. Grätzel, *Adv. Mater.* **17**, 813–815 (2005)
47. MdK Nazeeruddin, E. Baranoff, M. Gratzel, *Sol. Energy* **85**, 1172–1178 (2011)
48. V.K. Singh, B. Bhattacharya, S. Shukla, P.K. Singh, *Mater. Technol.* **49**, 123–127 (2015)
49. A. Nawaz, R. Sharif, H.-W. Rhee, P.K. Singh, *J. Ind. Eng. Chem.* **33**, 381–384 (2016)
50. P.M. Jayaweera, T. Sanjeewa, K. Tennakone, *Sol. Energy Mater. Sol. Cells* **91**, 944–950 (2007)
51. A. Hagfeldt, G. Boschloo, L. Sun, L. Kloo, H. Pettersson, *Chem. Rev.* **110**, 6595–6663 (2010)
52. X. Du, R. Fan, X. Wang, G. Yu, L. Qiang, P. Wang, S. Gao, Y. Yang, *Cryst. Growth Des.* **16**, 1737–1745 (2016)
53. Y.-S. Yen, J.-S. Ni, W.-I. Hung, C.-Y. Hsu, H.-H. Chou, J.-T. Lin, *Appl. Mater. Interface* **8**, 6117–6126 (2016)
54. T. Horiuchi, H. Miura, K. Sumioka, S. Uchida, *J. Am. Chem. Soc.* **126**, 12218–12219 (2004)